Femtosecond Spectroscopy of Halorhodopsin and Rhodopsin in a Broad Spectral Range of 400−1000 nm

Takayoshi Kobayashi,* Mijong Kim, and Makoto Taiji

Department of Physics, University of Tokyo, 7-3-1 Hongo, Bunkyo, Tokyo 113, Japan

Tatsuo Iwasa, Masashi Nakagawa, and Motoyuki Tsuda

Department of Life Science, Himeji Institute of Technology, Harima Science Garden, Hyogo 678-12, Japan

Received: February 26, 1997; In Final Form: October 17, 1997[⊗]

Femtosecond pump−probe spectroscopy of halorhodopsin from *Halobacterium halobium* and rhodopsin from octopus *(paroctopus defleini)* has been studied in a wide spectral range extending from 400 to 1000 nm. There are five common features to halorhodopsin and rhodopsin in the transient absorption and gain spectra. A comparative description of the primary photochemistries in the retinal proteins including bacteriorhodopsin is presented to explain the present experimental results systematically together with the previous studies. In the model there is a branching from the Franck−Condon state into coherent and incoherent channels. The former is the rapid process of direct formation of the first intermediate (bathorhodopsin for rhodopsin and hR_K intermediate for halorhodopsin), and the latter is the thermalization of the excited state in the retinoid proteins, from which slow formation of the first intermediate takes place.

I. Introduction

Rhodopsin consists of the apoprotein opsin and 11-*cis*-retinal chromophore. Absorption of a photon by rhodopsin triggers isomerization of 11-*cis*-retinal to all-*trans* form followed by the formation of a series of intermediates that initiate an enzyme casade resulting in the electric excitation.[1−5] The visual process in a photoactive cell consists of a series of chemical reactions via several intermediates ending by the culmination in the stimulation of an optic nerve. The *cis*−*trans* photoisomerization of the retinal is a well established primary process between the excited state in rhodopsin and the first intermediate. Several intermediates are proposed to exist in the early stage of the rhodopsin photoreaction,[6−10] namely primerhodopsin[11] (photorhodopsin[12]), hypsorhodopsin, and bathorhodopsin. However, in our previous work[13] we concluded that primerhodopsin, which is discovered by ourselves[11] and is equivalent to the photorhodopsin,[12] is simply a nonthermal bathorhodopsin and also that there is no strong evidence to claim the existence of hypsorhodopsin in the physiological process.

The appearance of the first intermediate in rhodopsin within 200 fs was first resolved by Schoenlein et al.[14] with 35-fs pump pulses centered at 500 nm and 10-fs probe pulses covering the spectral range between 450 and 580 nm. On the other hand, Yan and co-workers[15] subsequently presented a paper, in which they performed femtosecond experiments with the use of 400-fs pulses. They explained their results in terms of a sub-400-fs twisting process on the excited-state surface, which is followed by a 3-ps formation process from the excited-state to a ground-state photoproduct transition. Therefore, isomerization is concluded to be terminated within 200 fs in the former paper,[14] but it is claimed to take place with the time constant of 3 ps in the latter paper.[15] This controversial argument about the isomerization time had been unresolved.

In our previous work[13] of femtosecond pump−probe spectroscopy performed to solve the problem using octopus rhodopsins in H_2O and D_2O as samples, the probe light covered a much broader wavelength region of 400−1000 nm than those of other groups. Transient gain and absorption from the excited state of rhodopsin after 300 fs-pulse excitation were observed around 650 and 700 nm, respectively. Primerhodopsin, which was concluded to be a nonthermal bathointermediate, was formed within 400 fs from the excited state. Therefore, the *cis*−*trans* isomerization completes within 400 fs. Shank et al.[16] reported the observation of vibrational coherence in the photoproduct of the isomerization reaction in bovine rhodopsin. The presence of vibrational coherence in the photoproduct indicates that a nonstationary wave packet is carried along a nearly barrierless nonadiabatic surface from the excited state of the reactant to the ground state of the first intermediate photoproduct. Such a potential crossing between adiabatic potential curves and associated photochemical reaction is of great interest not only from the photobiological point of view but also from the viewpoint of femtochemistry. Even from our previous work it is not completely clear how the controversial argument about the isomerization time can be explained. To solve this problem we performed comparative study of halorhodopsin.

Bacteriorhodopsin (bR) and halorhodopsin (hR) in halobacteria both work for energy generation by light-driven proton and chloride pumps, respectively.[17,18] In both cases where the primary photochemical process triggered by a photon is the all-*trans* to 13-*cis* isomerization of a retinal molecule, the photochemical reaction of the pigments are closely related to the isomerization process from 11-*cis* to all-*trans* form in rhodopsin.

Halorhodopsin undergoes a cyclic reaction, which is initiated upon the absorption of a photon. The scheme of the photocycle

[⊗] Abstract published in *Advance ACS Abstracts,* December 1, 1997.

S1089-5647(97)00705-0 CCC: $15.00
Published on Web 01/01/1998

of halorhodopsin is as follows:[19] In the presence of chloride

$$hR\cdot Cl^- + h\nu \rightarrow hR_K\cdot Cl^- \rightarrow hR_{KL}\cdot Cl^- \rightarrow hR_L\cdot Cl^- \leftrightarrow hR_O\cdot Cl^- \rightarrow hR^{\bullet}\, Cl^-$$

An intermediate corresponding to the metarhodopsin of visual pigment does not appear in the protocycle.

In the absence of chloride, it is modified into

$$hR \xrightarrow{h\nu} hR'_K \rightarrow hR_{KO} \rightarrow hR_O \rightarrow hR$$

The energy input by the absorption of a photon takes place strictly at the first step only, and all subsequent relaxation processes are thermally driven back to the original state. The absorption spectrum of halorhodopsin in the stationary state shows a maximum at 578 nm. The first identifiable intermediate reported on the picosecond-time scale is hR_K, which absorbs light near 600 nm.[20−22] There hR_K is converted into hR_{KL} absorbing light around 565 nm, in less than 60 ns,[23] and hR_L is generated from hR_{KL} with a rise time of 0.46 μm.[24] The absorption spectrum of hR_L has a peak at 526 nm. The hR_L is in a chloride-dependent equilibrium with hR_O, which absorbs light at 635 nm. Kinetic simulations of the $hR_L \leftrightarrow hR_O$ equilibration during the photocycle at different chloride concentrations identified the $hR_L \rightarrow hR_O$ reaction as a reaction accompanied by the release of chloride ions.[25,26] To balance this loss of chloride, chloride uptake is postulated to take place before the absorption of the next photon.[27]

Even though considerable advance in picosecond laser spectroscopy had been made, only two groups reported primary photoprocesses in halorhodopsin.[20−22] They suggested that the possible existence of the J-intermediate (hR_J) and that the relaxation (directly) from the excited state to the ground state competes with isomerization of retinal. Their experiments were performed over a limited wavelength region, 400−780 nm, with a time resolution of 0.6 ps.

In the present paper we have studied femtosecond spectroscopy of halorhodopsin and rhodopsin and revealed a resemblance in the transient transmittance (absorption, gain, and bleaching) spectra and the femtosecond to picosecond dynamics. Especially the appearances of two gain spectra are of much interest in the shorter and longer wavelength regions with shorter and longer lifetimes, respectively, and of the excited-state absorption in the spectral region between them. From the results we propose a scheme to explain the experimental results and solve the problem of the controversial arguments about the results of rhodopsin between the two groups.[14,15]

II. Experimental Section

A. Femtosecond Spectroscopy Apparatus. The femtosecond transmission spectrum was studied with a colliding-pulse mode-locked (CPM) dye laser with a four-stage dye amplifier system. The dye amplifier is pumped by the second harmonic of a Q-switched Nd:YAG laser. The center wavelength and duration of the amplified pulses are 628 nm (corresponding to the photon energy of 1.92 eV) and about 100 fs, respectively. The amplified fundamental was used as an excitation pulse source for halorhodopsin experiment. A spectral region around 526 nm is selected from the femtosecond continuum generated by a part of the amplified CPM laser, and it was amplified by the third harmonic of another Q-switched Nd:YAG laser to be used as an excitation source of rhodopsin experiment. The femtosecond continuum generated by the rest of the amplified CPM laser was used as a probe light for rhodopsin experiment.

B. Halorhodopsin Sample. Isolation of halorhodopsin was followed by the established procedure.[28] *Halobacterium halobium* strains OD-2W and L-33, which lack bacteriorhodopsin but contain halorhodopsin and other bacterial retinal proteins, were grown at 39 °C in the growth medium that contained the following components per liter: 250 g of NaCl, 20 g of $MgSO_4\cdot 7H_2O$, 3 g of sodium citrate, 2 g of KCl, and 10 g of oxoid peptone. Aeration was performed at 2.5 L/min for the first 3 days, and 1.5 L/min for the rest of the growth period.

The harvested cells were washed once with 4 M NaCl and dialyzed overnight at 4 °C in the presence of a few micrograms of DNase type I against a large volume of distilled water. The reddish-purple membranes were recovered by centrifugation at 105 000*g* at 10 °C for 60 min and washed once with 320 mL of NaCl and 25 mM Tris·Cl, pH 7.2. The washed membranes were suspended in 120 mL of the same buffer, solid NaCl was added to bring the salt concentration to 4 M, and $^1/_3$ volume of 20% (w/v) sodium cholate was added. All subsequent steps were carried out at room temperature under dim illumination. A clear purple-red supernatant was separated by centrifugation as above. The supernatant was introduced onto a 2.5 × 15-cm column of phenylsepharose previously equilibrated with cholate buffer (4 M NaCl, 25 mM Tris·Cl, pH 7.2, 0.4% sodium cholate), and washed with 2 L of the cholate buffer. Then the halorhodopsin was eluted with about 500 mL of the buffer (4 M NaCl, 25 mM Tris·Cl, pH 7.2, 0.5% octylglucoside). The solution was introduced onto another phenylsepharose column of 2.5 × 4-cm size, equilibrated with cholate buffer, as before. Washing with 500 mL of cholate buffer was followed by elution with the octyl glucoside buffer, as before. The final products were suspended in 1% octyl glucoside buffer (0.5 M NaCl, 10 mM 3-(*N*-morpholino)propanesulfonic acid, pH 7.0). Sample suspension was kept in a 1-mm thick fused silica cell in order to avoid the influence of the surface ion of the glass cell.

All the experiments were performed at room temperature (22 °C).

C. Octopus Rhodopsin Samples. The microvillar membranes of the octopus retina (Mizudako, *paroctopus delfeini)* were isolated by sucrose flotation (34 wt %, buffer A) (400 mM, KLC, 10 mM $MgCl_2$ + *p*-APMSF) repeated twice. The obtained pellet was washed several times with buffer A and with buffer B (10 mM MOPS [pH 7.4], 1 mM DTT, 20 μM *p*-APMSF). The final products were suspended in the buffer B and kept at −80 °C in the dark. A part of this frozen sample was thawed and centrifuged. The pellet was solubilized in H_2O with 2 mM MOPS [pH 7.4] and 2% sucrose monolaurate (L-1690 or SM-1200). The solution was centrifuged and the supernatant was used as a sample. Three different samples a, b, and c of octopus rhodopsin were prepared to see the reproducibility of the experimental results. The peak absorbances of a, b, and c in a 1-mm cell are 0.8, 1.2, and 1.3, respectively. The detergent used is L1690. Deuterated membranes obtained by freeze-drying from suspension in D_2O were also used as a sample. This procedure was repeated three times for complete deuteration. The peak absorbance of the sample d in D_2O is 1.5.

The samples were contained in a 1-mm thick cell, and the temperature of the 250-μL samples was kept constant at 8.0 ± 0.5 °C. After about 150-shots excitation, rhodopsin was irradiated with the halogen lamp (Hoya-Schott, HL100R) through cutoff filters (Hoya, O58 and HA30) to convert any acid metarhodopsin back to rhodopsin. Fractions of less than 5% of the samples were bleached by the 150 shots excitation.

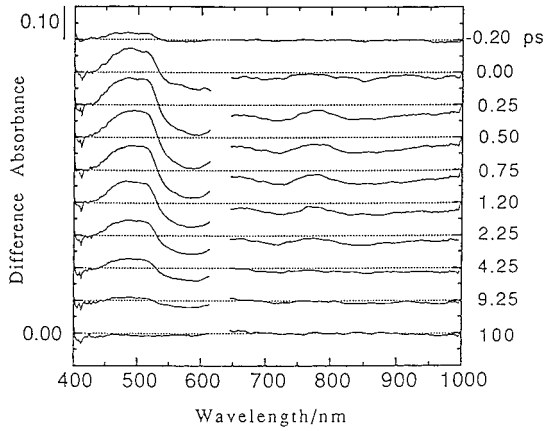

Figure 1. Difference transmission (absorption, gain, and bleaching) spectra of halorhodopsin in the unit of absorbance at several delay times. The data are not displayed in the wavelength region of 615−645 nm because of disturbance due to the scattered pump light at 627 nm.

III. Results and Discussion

A. Femtosecond Difference Absorption Spectra of Halorhodopsin. Figure 1 shows the difference transmission (absorption, gain, and bleaching) spectra of halorhodopsin at several delay times. The difference absorption spectra are averaged over delay time intervals as follows: ±0.05 ps for 0.0, 0.25, 0.5, 0.75, and 1.20 ps; ±0.1 ps for −0.20 ps; ±0.20 ps for 2.25 ps; ±0.50 ps for 4.25 and 9.25 ps. The spectrum at 100 ps is not averaged over a time interval. The data in the 615−645 nm region are not displayed because of unavoidable disturbance due to the scattered pump light at 628 nm. There are five clear features in these spectra, which are summarized as follows: (1) the prominent broad induced absorption around 500 nm due to the transition from the excited state, (2) the bleaching with a peak around 580 nm, (3) the gain in the broad spectral region of the wavelengths longer than 650 nm, (4) weak absorption around 670 nm attributed to hR_J in the previous papers, (5) the convex feature around 760−780 nm, and (6) a very weak but reproducible induced absorption around 650 nm at longer delay times than 10 ps. Most of these features resemble those of rhodopsin, which will be discussed later.

B. Time Dependence of the Transient Absorbance Change. Figure 2 shows the time dependence of the transmittance (absorbance or gain) change at various wavelengths. They are obtained by averaging over probe spectral regions of ±5 nm width centered at wavelengths. The probe wavelengths of 470, 490, and 510 nm are located in the region where the induced absorption is observed.

The bleaching due to the ground-state depletion at 550, 570, and 610 nm and the absorption due to the batho product at 650 and 670 nm are detected as will be discussed below. Negative signals due to the gain are observed at 700, 720, 820, and 870 nm.

The time constants in a wavelength region between 450 and 900 nm are determined by fitting with a single-exponential function and a constant term corresponding to a species with much longer delay time constant than 100 ps. In 450−520 nm, the induced absorption decays with a time constant of 3.5−4.0 ps. In 540−610 nm, the bleaching disappears with time constants of 3.5−3.8 ps. The time constant becomes shorter to be 2.3 ± 0.2 ps at 530 nm, which is not shown in Figure 2. This shortening is because of the cancellation of the difference absorption signal due to the excited state in halorhodopsin with that due to the ground-state depletion that takes place in this

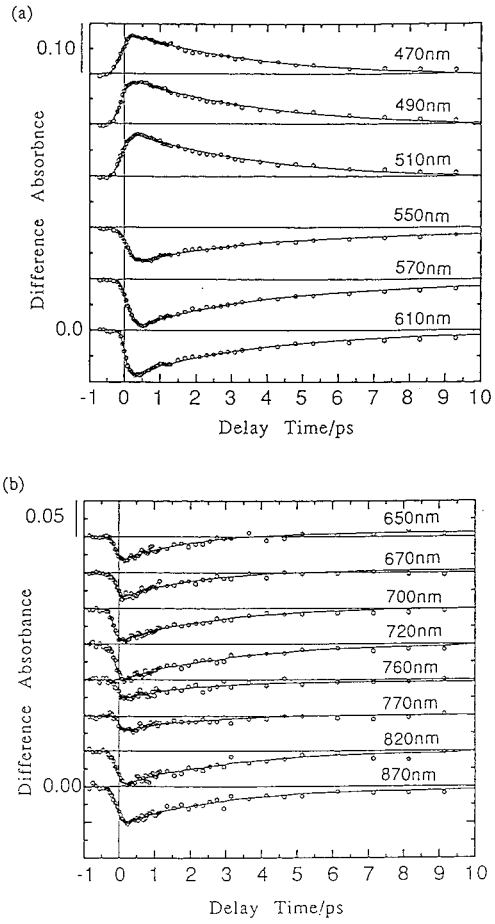

Figure 2. Transient absorbance change in halorhodopsin after femtosecond-pulse excitation. The signals are averaged over the spectral region of 10 nm centered at wavelengths in the figure. The experimental results are shown as circles. The data are fitted with single-exponential functions (solid lines).

spectral region. Decay time constant in the wavelength region longer than 650 nm depends on the wavelength unlike those of 450−610 nm. It is between 2.1 and 2.5 ps in the region of 650−700 nm, gradually increases in 680−720 nm to be 3.4 ± 0.2 ps at 720 nm, then gradually decreases in 720−760 nm to be 2.0 ± 0.3 ps at 760 nm, increases again in 760−790 nm to become 3.2−4.1 ps in 790−860 nm, and then decreases again to 2.7−2.9 ps in 870−900 nm.

From the location of the ground-state absorption spectrum, three components are expected to be seen around 650 nm in Figure 2: negative signals due to the ground-state depletion of halorhodopsin which is not recovered until the full photocycle is terminated, another negative signal due to the stimulated emission from the excited-state halorhodopsin, and a positive signal of the induced absorption due either to the photoproduct or to the excited state of halorhodopsin. The ground-state halorhodopsin has the absorption spectrum of which the maximum is located around 580 nm with a fullwidth of about 100 nm, corresponding to the bleaching observed in the spectral range in Figure 1. The spectrum of the bathoproduct of halorhodopsin has a maximum around 600 nm, and its fullwidth at half-maximum is about 80 nm.[29] From the above consideration the time evolution of the absorbance change ΔA_{650} observed around 650 nm can be fitted with a sum of two exponential functions and a constant term convoluted with the instrumental function in the form of sech^2 for both the pump

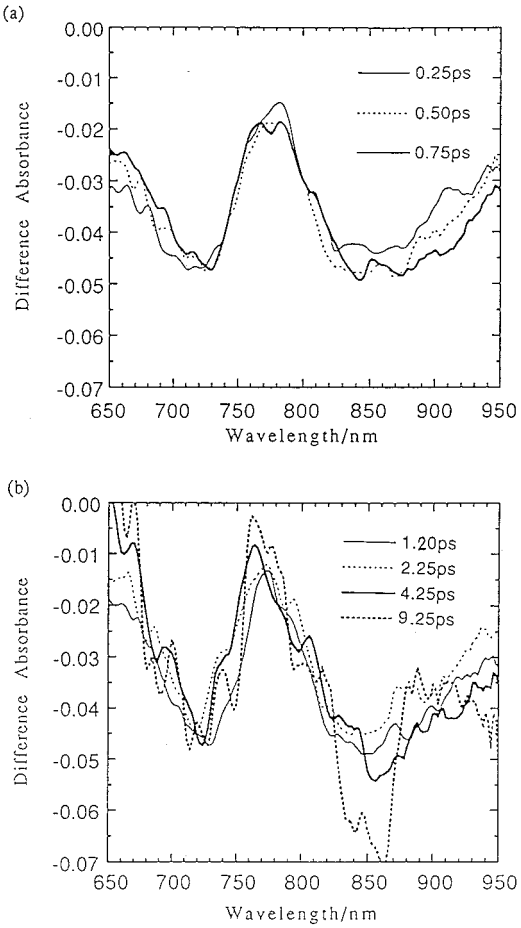

Figure 3. (a) Normalized difference transmission spectra of halorhodopsin by the negative peak signal around 720 nm at 0.25, 0.50, and 0.75 ps after excitation. The signals are averaged over ±0.05 ps delay time. (b) Normalized gain spectra of halorhodopsin at 1.20, 2.25, 4.25, and 9.25 ps after excitation. The signals are averaged over the delay time intervals as follows: ±0.05 ps for 1.20 ps, ±0.20 ps for 2.25 ps, ±0.50 ps for 4.25 and 9.25 ps.

and probe pulses with 0.25 ps fwhm as follows:

$$-\Delta A_{650} = \{A_1 \exp(-t/\tau_1) + A_2(1 - \exp(-t/\tau_2)) + A_3\} \otimes F(t) \quad (1)$$

Here pre-exponential factors, A_1 and A_2, are proportional to the respective absorbance changes and A_3 corresponds to the constant term due to the long-lived component. The first term represents the decay process of the negative signal, corresponding to the two processes of partial bleaching recovery and the gain dynamics with the common rate constant of $1/\tau_1$. The second term represents the decay due to the formation of the intermediate from the excited state of the photoproduct, with the formation rate constants of $1/\tau_2$. The time constants τ_1 and τ_2 are determined to be 3.5 ± 0.9 ps and 1.1 ± 0.6 ps, respectively, at 650 nm.

C. Excited State in Halorhodopsin. Figures 3a,b shows gain spectra at several time delays (a) shorter and (b) longer than 1 ps. They are averaged over some delay time intervals as follows: ±0.10 ps for −0.20 ps, ±0.05 for the signals at 0.0, 0.25, 0.50, 0.75, and 1.20 ps; ±0.20 ps for 2.25 ps; ±0.50 ps for 4.25 and 9.25 ps. Just after the excitation, a small but reproducible spectral red shift of the bleaching can be observed up to 0.75 ps as shown in Figure 3a, while almost no clear change in spectral shape takes place after 0.75 ps as shown in Figure 3b.

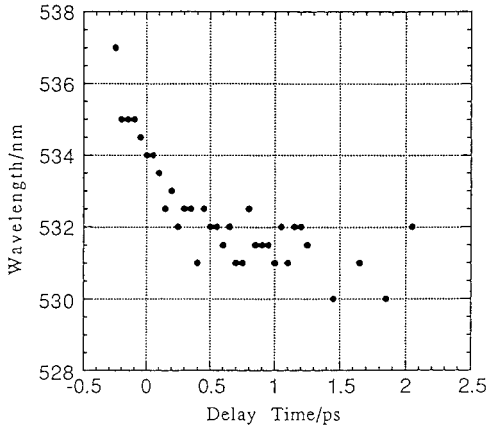

Figure 4. Decay time constants of the transient absorbance change observed in various spectral regions. The spectra are averaged over the spectral region of 10 nm centered at wavelengths in the figure. The time constants are the result of single-exponential fitting. Because of the poor signal to noise ratio, time constants only in the wavelength region of 450−900 nm are shown.

Figure 1 shows the positive absorbance change due to induced absorption peaked at about 480 nm and the negative absorbance change due to the gain and absorption depletion peaked at about 590 nm. The wavelength of zero absorbance change between these positive and negative signals shift to blue as shown in Figure 4. The origin of this shift can be considered as follows. The absorption spectrum of halorhodopsin in the ground state is inhomogeneously broadened because of a large number of possible conformational substates in the halorhodopsin protein. Since the pump pulse (628 nm) is resonant on the longer wavelength edge of the broad absorption spectrum, lower energy substates are more likely to be excited. Therefore, the spectral change observed corresponds not to the energy transfer among the *inhomogeneous* groups but to the energy relaxation taking place in the *homogeneous* groups located energy at the bottom of the inhomogeneous distribution. Only a small blue shift of 6 nm was observed for the induced absorption due to the lowest excited singlet (S_1) state in halorhodopsin from −250 fs to +500 fs. The blue shift is due to the flatter potential curve of the S_n state (final state of the S_1 state absorption) than that of S_1 state. The spectral shift and the features potential curved deduced from the ultrafast time-resolved data are the same as those of rhodopsin.[13−16]

D. Bathoproduct of Halorhodopsin. The absolute spectrum of batho-like product hRJ was calculated by Zimányi et al.[25] and Tittor et al.[29] with the aid of absorption spectroscopy at 140 K and flash photolysis, respectively. The spectrum shows a broad band with a peak at 598 nm and a full width at half-maximum of 82 nm. In the present experiments, the net absorption due to the bathoproduct is detected only around 650 nm because it is overlapped with the bleaching. By Fourier transform infrared spectroscopy,[30] Rothschild et al. suggested that the bathoproduct has a 13-*cis*-retinal.[31]

From the temporal dependence of the induced absorption at 650 nm discussed above, and those at other wavelengths, the formation time constant of the bathoproduct is estimated as 1.0 ± 0.6 ps, which corresponds to the isomerization process all-*trans* → 13-*cis*. The formation time is substantially shorter than the decay time constant of the excited-state halorhodopsin of 3.4−4.0 ps. If the isomerization occurs from the relaxed excited state, the rise time of absorption at 650 nm is expected to be equal to the decay time of the excited state. The experimental result implies that the isomerization process is not from the relaxed excited state. Similar femtosecond spectroscopic results

of halorhodopsin were reported by Kandori et al.[20] They determined the rise and decay times from the kinetic simulation on difference absorption spectra at 646 nm. Their rise time of the bathoproduct was estimated to be slightly shorter than 1 ps using a femtosecond apparatus with 0.6 ps resolution,[22] which corresponds to 1.0 ± 0.6 ps in the present experiment.

Even though metarhodopsin is not involved in the halorhodopsin photocycle as mentioned in the Introduction, the rest of the species, such as $hR_{O'}$, were observed, and their kinetics resemble those of the intermediates of the bacteriorhodopsin photocycle. The rise time of batholike product, hR_J, is also similar to that of bR_J,[32−35] which is formed from bR_I (with a time constant of 500 fs) and then converts to bR_K (3 ps). Isomerization is expected to take place during the $bR_I \rightarrow bR_J$ process. From the comparison with the absorption peaks of bR, bR_J, and bR_K, the absorption peak of hR_K is expected to be red-shifted and blue-shifted from those of hR and hR_J, respectively. In the present experiment, a net positive absorbance change around 640−650 nm due to hR_K could not clearly be detected. This is simply due to the cancellation by the bleaching of the ground-state absorption.

Although there are such resemblances, it is possible that the primary photoprocesses of halorhodopsin and bacteriorhodopsin have some differences since they contain different protein moieties. The lifetime of the excited-state bacteriorhodopsin is 500 fs, while the excited halorhodopsin decays with a time constant of 3.5 ps. It was reported that the hypsoproduct of halorhodopsin is formed at 80 K under various illumination while under the same conditions only bR_K appears in bacteriorhodopsin by Zimányi and others under the same conditions.[36] This may be explained by the possible opening of a new channel to the hypsointermediate during the long lifetime of the excited state in halorhodopsin.

E. Two Induced Absorption Bands Due to the Excited-State Halorhodopsin in Visible Wavelength Region. The spectra normalized at the downward peak around 720 nm are shown in Figure 3a,b to see a time dependence of the spectral change in 650−900 nm. The amplitude of the upward peak around 770 nm becomes smaller up to 0.75 ps as shown in Figure 3a, and it grows over 1.20−9.25 ps in Figure 3b. This implies that at least two components exist in the region >700 nm. There are three possibilities to be considered to explain the upward peaking structure in 720−850 nm region shown in Figures 3a,b and the differences in time constants at 760 and 770 nm from those at the other wavelengths shown in Figure 5: (1) There are two gain processes in the shorter and longer wavelength regions. They overlap around 770 nm. (2) There are a single broad-band gain in the longer wavelength region of 700−950 nm and a relatively narrow absorption band in 750−800 nm. (3) The positive peaking around 760−770 nm may be due to impulsive Raman process discussed by Pollard and others.[37] If the gains are of different origins (case 1), two different time constants of gain are expected to be observed, and the overlapped region would have a different time constant from the two because of the close values of the time constants. However, the two gain regions are observed to have almost the same time constants, and the time constants in the overlapped region are shorter than the common decay time. Thus case 1 is ruled out.

The impulsive Raman is expected to exist only within the vibrational dephasing time. However, the positive peaking signal lasts as long as 9 ps or even longer. The impulsive Raman process can give rise to hot ground-state populations that may exist for several picoseconds. Such hot ground state

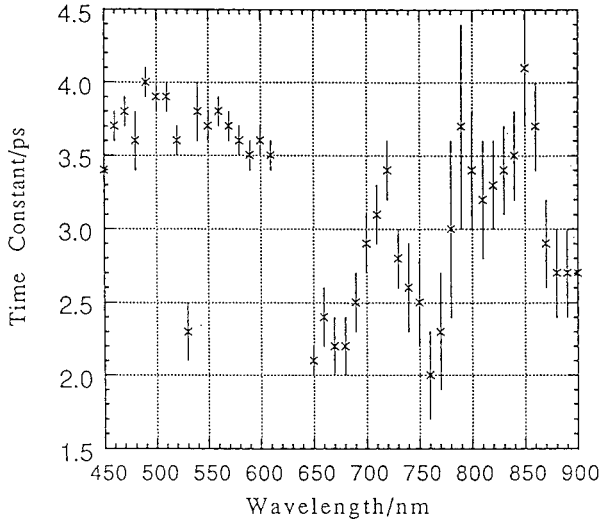

Figure 5. Spectral shift of the wavelength of zero absorbance change in the transient spectra of halorhodopsin in the course of delay time.

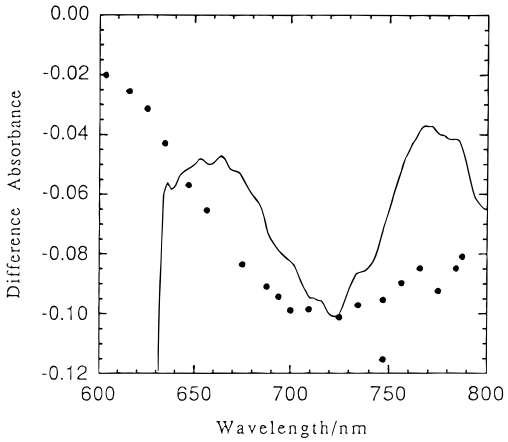

Figure 6. Calculated gain spectrum (closed circles) from the fluorescence spectrum in the literature[20] and an average of difference absorption spectra (solid line) of halorhodopsin at delay times of −0.2, 0.25, 1.2, and 4.25 ps. The sign of the calculated gain spectrum is inverted to compare with the sum of gain spectrum.

are typically-observed as an induced absorption that is red-shifted from the normal ground-state absorption. The feature discussed here is a sharp positive peaking that is far from the ground-state absorption. Therefore, case 3 as an explanation of the positive peaking around 760−770 nm can also be eliminated, and hence case 2 is most probable.

Closed circles in Figure 6 show the gain spectrum, $G(\lambda)$, that is calculated by using the relation $G(\lambda) = F(\lambda)\lambda^4$ from the fluorescence spectrum, $F(\lambda)$, measured by a streak camera with a time resolution of 3 ps by Polland et al.[21] The solid line shows the spectrum of a sum of gain spectra at −0.2, 0.25, 1.2, and 4.25 ps. The spectra do not coincide exactly with each other, but both of them have a peak at approximately 720 nm. The deviation in the shorter wavelength region could be explained by the induced absorption due to the bathoproduct.[25,29] The broader feature of the calculated spectrum from the stationary fluorescence is probably because the latter is contributed from both relaxed and nonrelaxed states while the observed time-resolved spectrum is contributed only from the nonrelaxed one.

To isolate the induced absorption, the gain is supposed to have a flat spectrum over the spectral region of 720−840 nm. The gain spectrum is obtained by assuming a single-exponential decay function with a time constant of 4.5 ± 0.7 ps. It is worthwhile to point out that the rise time of the induced

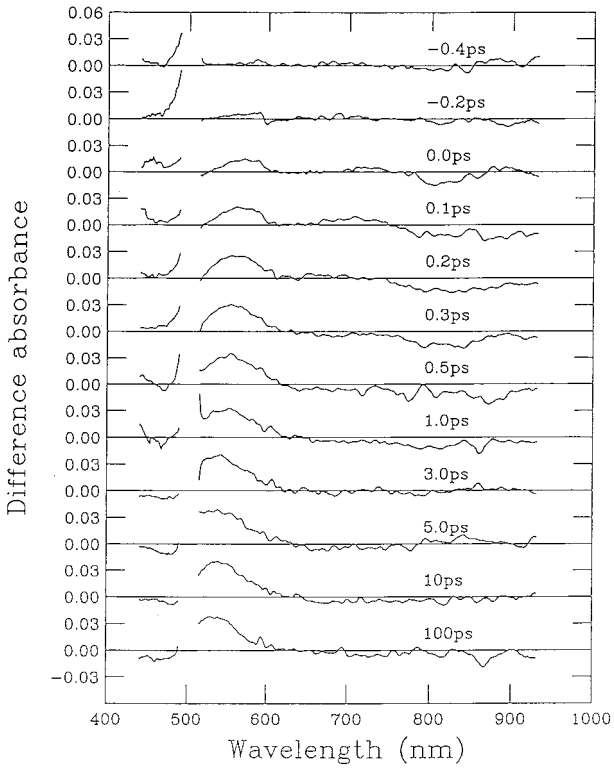

Figure 7. Difference absorption spectra of octopus rhodopsin in H_2O at 8 °C. Delay times between pump and probe pulses are shown in the figure.

absorption was shorter than resolution time of 100 fs. If the induced absorption at 770 nm is due to another photoproduct, a rise time is expected to be detected, and it should correspond to the dynamics of the photoproduct. On the basis of this observation, the induced absorption is also due to the transition from the S_1 state to the higher excited singlet states S_n's.

Tallent and his collaborators reported a theoretical study of the dynamics of the $S_n \leftarrow S_1$ absorption spectrum in rhodopsin.[38] The primary photochemical reaction in rhodopsin involves an 11-*cis* to all-*trans* photoisomerization retinal chromophore. They suggested the existence of two absorption bands in the $S_n \leftarrow S_1$ absorption spectrum in 0−325 fs. One has an absorption maximum around 340 nm, and the other is centered between 540 and 580 nm. The latter is associated with the transition into the excited singlet states of S_3 and S_4. They also suggested that an absorption appeared in the wavelength region around 780 nm after 375 fs, which was diagnostic of the $C_{11}{=}C_{12}$ dihedral angles in the region $80° < \phi_{11,12} < 100°$.

The stationary absorption maximum of rhodopsin is near 500 nm, while that of halorhodopsin is 578 nm. By taking into account the spectral shift, the induced absorption spectra of halorhodopsin around 430−520 and 720−840 nm are considered to correspond to the absorption bands around 320 and 560 nm, respectively, due to the excited rhodopsin, because both absorptions in the excited-state halorhodopsin are reproducable by fitting with a single-exponential function. The induced absorption over 720−840 nm was separated by the fitting to the decay functions composed of three components in eq 1.

F. Femtosecond Difference Absorption Spectra of Octopus Rhodopsin. Figure 7 shows difference absorption spectra of octopus rhodopsin in H_2O (sample c) and D_2O (sample d) at several delay times. The spectrum in the 505−540 nm region could not be measured because of a disturbance due to very strong scattered pump light at 525 nm. To reduce the scattered pump light, a notch filter was used, and this also reduces the probe light intensity resulting in the low signal-to-noise ratio in the 400−500 nm region. It is also because of the reduced probe light intensity by strong stationary absorption in the region more severely than in the longer wavelength region.

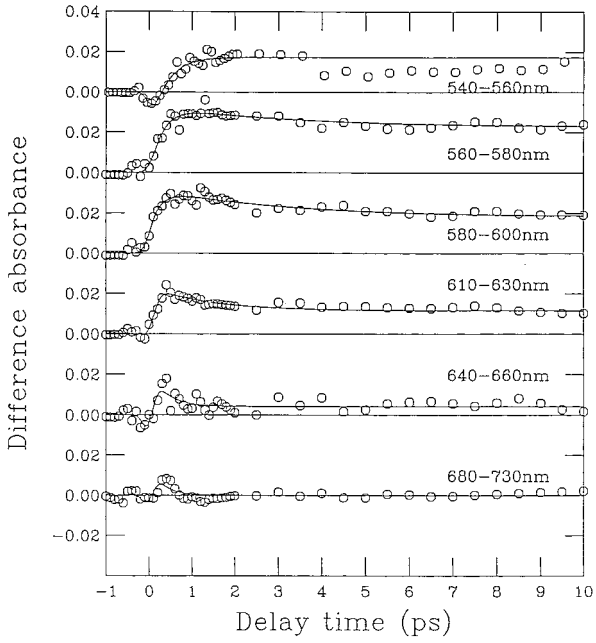

Figure 8. Delay time dependence of difference absorbance after femtosecond pulse excitation of octopus rhodopsin sample b in several probe wavelength regions between −1 and 10 ps.

There are five features in the spectra: (1) bleaching in the region around 500 nm, (2) prominent induced absorption around 580 nm, (3) small gain in the region of 630 rim around time zero, (4) very small but reproducible induced absorption around 700 nm, and (5) gain in the broad spectral region of 800 nm. All these features were also observed in all three other samples, samples a and b in water. Sample d also has all the above characteristics except with about a 10-nm red shift of whole spectrum.

The time dependence of the absorbance change of the samples a and b is depicted in Figures 8 and 9, respectively. They were integrated over appropriate spectral regions to achieve a higher signal-to-noise ratio. The data were fitted with a decay function composed of the sum of two exponential functions convoluted with a Gaussian pulse shape representing the finite pulse width of pump and probe. The experimental results are summarized as follows.

At first, the induced absorption in the 680−730 nm and 640−660 nm regions appear within 100 fs, and the former and the latter decay with time constants of 140 ± 70 fs and 360 ± 180 fs, respectively, for sample b in H_2O. Though it is difficult to determine a rise time because of limited time resolution, it seems to take finite time of the induced absorption to grow because there are always some negative absorption due probably to gain just after excitation before the induced absorption starts to grow at negative delays in these wavelength regions. Doukas and his collaborators measured the fluorescence spectrum from squid rhodopsin that has a peak around 630 nm and estimated its decay time as 120 ± 50 fs from the very low fluorescence quantum yield of 1.2×10^{-5} and the natural lifetime of 10 ns determined by the absorption spectrum.[39] Therefore the nonthermal stimulated emission from the state, which is not substantially relaxed from the Franck−Condon state, could be the origin of such a short-lived signal. The similar time constants of about 100 fs were observed for structural changes of one-dimensional systems

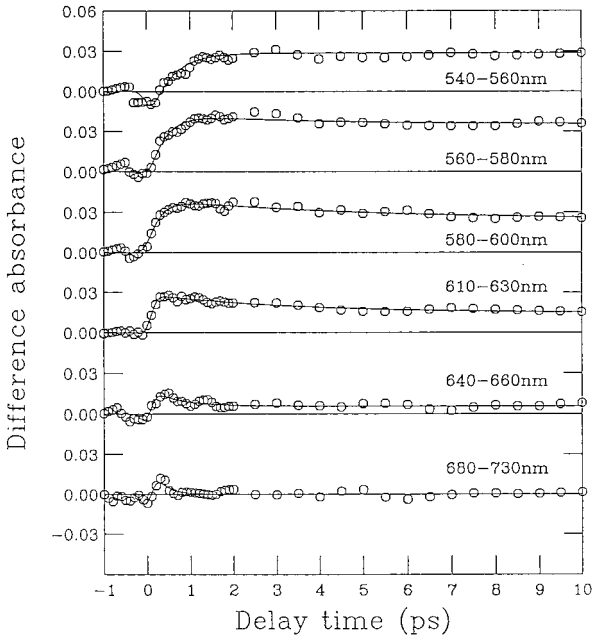

Figure 9. Delay time dependence of difference absorbance after femtosecond pulse excitation of octopus rhodopsin sample d in several probe wavelength regions between −1 and 10 ps.

of conjugated polymers such as polydiacetylenes with strong electron−phonon coupling.[40,41] These polymers are also considered to have a barrierless potential curve between the bottoms of the free excitor and the self-trapped exciton.[40,41]

The induced absorption observed in the 640−730 nm region is considered to be due to the excited-state of rhodopsin, since it grows up within 100 fs. The faster decay time that occurred at longer wavelengths (∼700 nm) rather than at shorter wavelengths (650 nm) as shown in Figures 8 and 9 can be explained by the redistribution of vibrational energy in the excited state. In the longer wavelength region, the absorption form the excited state near the Franck−Condon state is dominant, but in the shorter wavelength region the contribution from the relaxed excited state becomes larger. The decrease in the absorbance change in the longer wavelength region is due to depopulation of the Franck−Condon state in which thermal equilibrium is not yet attained even among various vibrational modes. In the meantime, the energy of the torsional motion of the retinal chromophore around the C_{11}=C_{12} double bond is released to other low-frequency modes such as bending modes. This energy redistribution makes the initial wave packets diffuse because of the increased inhomogeneous width, resulting in the blue shift of transient absorption spectrum. Therefore, slower relaxation time was observed in the shorter wavelength region.

In the 540−600 nm region, the most prominent induced absorption was observed. The rise time of the induced absorption is estimated to be in the range of 200−400 fs depending on the probe wavelength, which nearly coincides with the decay time in the 640−730 nm region. Similar femtosecond spectroscopic results of bovine rhodopsin were reported by Schoenlein et al.,[14] but it was difficult to identify the relaxed excited state. In bacteriorhodopsin, the relaxed excited state is considered to have strong induced absorption around 460 nm.[33,34,42] In octopus rhodopsin, we could not find any strong induced absorption in 420−460 nm. This may be due to the ultrafast nonadiabatic transition.[4] If the transition is fast enough, the adiabatic crossing can take place without passing through the relaxed excited state.

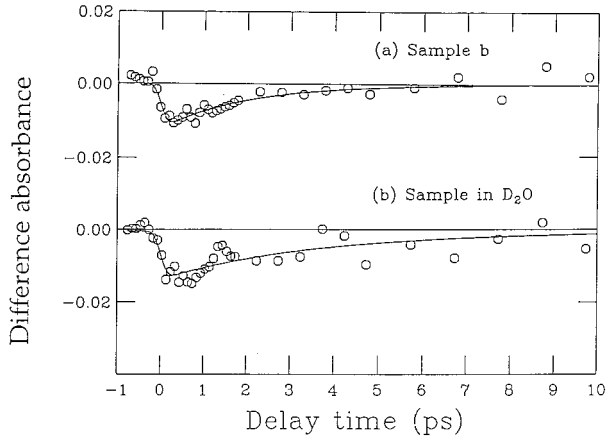

Figure 10. Delay time dependence of difference absorbance after femtosecond pulse excitation of octopus rhodopsin in H_2O in the spectral region of 860−920 nm. The fitted decay times using the data up to 100 ps not shown in this figure are 2.2 ± 0.8, 2.3 ± 0.5, and 4.0 ± 1.5 ps, for (a) octopus rhodopsin in H_2O and (b) octopus rhodopsin in D_2O, respectively.

The most interesting and puzzling result obtained is the gain spectrum at the longer wavelength region. The origin of the gain in >850 nm may be assigned to the relaxed excited state. However, the photon energy of the emission (∼900 nm, corresponding to 32 kcal/mol) seems to be too high to be attributed to the emission from the relaxed excited state since the energy was estimated to be about 5 kcal/mol by quantum chemical calculations.[38] If the origin of the emission is not a relaxed excited state but states on the way to relaxation, its large photon energy can be explained.

The origin of the gain in the wavelength region longer than 850 nm may at first sight be explained to be due to the stimulated emission from photoproducts of rhodopsin. In this case the excitation power dependence is expected to be superlinear. However, the dependence of the signal averaged over 805−957 nm is found to be linear within experimental error; therefore, a contribution from photoproducts is concluded to be negligibly small. We also measured samples containing detergent only, but no signal was detected. This fact indicates that the origin of the gain is surely rhodopsin in the excited state. Figure 10 also shows that the decay time of the gain spectrum integrated over 860−920 nm is determined to be 2.0 ± 0.8 ps in sample c and 4.0 ± 1.5 ps in sample d.

Very recently it was reported[43] that there is a very short-lived component with shorter life than ∼100 fs in the photoisomerization process in bacteriorhodopsin. It has two gain regions just below the bleaching due to the ground-state depletion and above the absorption band due to the J-intermediate (bR_J) of bacteriorhodopsin. This apparent discrepancy between the gain decay time (≤100 fs) and the rise time (∼200 fs) of the first intermediate J is the same situation as observed in the present study and previous studies.[13−15,44]

From these experimental results and the discussions made earlier, we would like to propose a model to explain the coexistence of the long-wavelength gain with much longer lifetime than the formation time of the first intermediates, namely, nonthermal bathorhodopsin in octopus rhodopsin, primerhodopsin which is attributed to be hot (or more appropriately nonthermal) bathorhodopsin intermediate, and J-intermediate, which is also hot (nonthermal) K intermediate in bacteriorhodopsin.

As in rhodopsin, very fast formation of the first intermediate takes place before thermalization, namely, within 200 fs after

excitation. Even a vibrational coherence is still existing in the first intermediate.[14,16,44] However, the modulation depth in the absorbance due to the vibration is only less than 20% at most in all the wavelengths observed.[14,16,44] This means that the energy dissipation from the initially prepared vibrational state occurs quickly (probable transitional motion around the C_{11}═C_{12} double bond but strongly coupled to the photoexcited S_1 state in rhodopsin). The wave packet does not come back to the same minimum of the upper adiabatic potential curve near the twisted configuration, since the potential curve is not as simple to be depicted in a single-dimensional configuration space along the torsional (isomerization) angle around the C_{11}═C_{12} double bond. In this case the effective nuclear velocity ν component along the torsional coordinate near the crossing region on the potential curve is reduced. Then the Landau−Zener tunneling probability[45,46] given by $P \sim \exp(-1/\nu)$ is sensitive to ν and is expected to be substantially reduced in a multimode system.[47]

After the first crossing to the first nonthermal intermediate in the ground electronic state, the residual rhodopsin in the excited electronic state (S_1) will experience the spread of the wave packet and stays there for 2 and 4 ps in H_2O and D_2O, respectively, because of reduced crossing rate induced by the wave-packet spreading. Meanwhile it will relax to the ground state of rhodopsin by a very efficient nonradiative process because of the very small difference in energy between the excited state and the ground state. At the same time it emits spontaneous fluorescence in the spectral region of 900 nm with the estimated efficiency of $<10^{-4}$ from the natural lifetime and the observed decay time of the gain. Only the value of the upper limit can be obtained since the radiative life or natural lifetime from the S_1 state in the related configuration is expected to be longer than that obtained from the ground state because of a reduced radiative coupling due to a very large geometrical configurational change in the S_1 state. It may also possible that this process also feeds the thermal bathointermediate, which is depicted in the exponential tail of the Boltzmann distribution observed in the spectral region as shown in Figure 7.

The experimental results of fast gain decay (100 fs) and slower J-intermediate formation (200 fs) obtained by Gai et al.[43] can be explained as follows. The earlier very rapid process can be explained by the very fast population decay and rapid red shift of the gain both associated with the approach of the reactant to the potential crossing region. The later slower process is the main process of the population of the J-intermediates.

There are two important subjects to be studied in the near future to verify the model proposed in the present study. One of them is the detection of the slow growth of the small formation of the bathointermediate corresponding to the long-lived excited state exhibiting the slow gain process. The other is the observation of the spontaneous fluorescence in the longer wavelength corresponding again to the long-lived excited state.

From the consideration including other retinoid proteins, the ultrafast processes in the rhodopsin family may be summarized as shown in Figure 11. In the primary processes in all retinoid proteins, there is branching from the Franck−Condon excited state indicated by the double asterisk (**) and the subscript fc to two channels. One channel is to the fast formation of the first intermediates that are not thermalized. They are indicated by "hot" but they may be a nonthermal state or thermal state with higher temperature than the lattice (bulk) temperature. During this process coherence, of vibration associated with the isomerization is partially maintained.

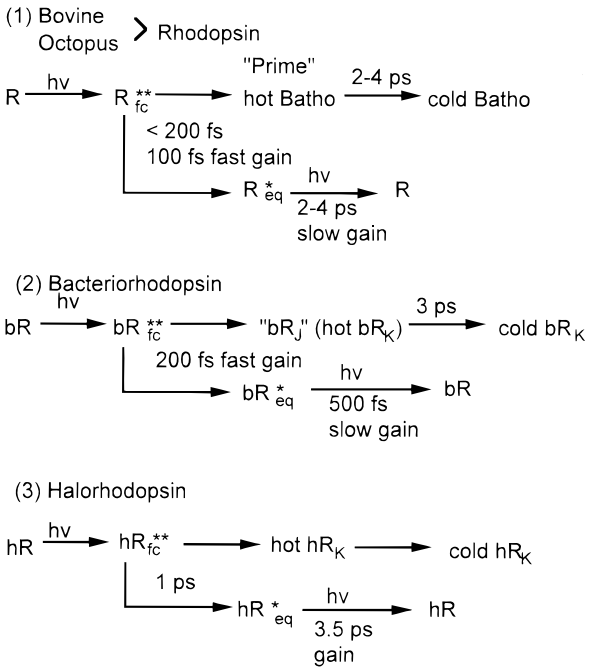

Figure 11. Summary of the ultrafast processes in the retionoid proteins.

The other channel is to the equilibrium state in the lowest excited state S_1 of each retinoid protein. There may be a slow formation process from this thermal excited state to the first intermediate in a thermal equilibrium state. In this process the vibrational coherence is lost. Therefore, the former and the latter processes may be called coherent and incoherent formations of the first intermediates.

In conclusion, by comparative study of femtosecond spectroscopy of halorhodopsin and octopus rhodopsin, we proposed a model of branched process in the primary state of the photochemistry in retinoid proteins, namely, coherent (ballistic) and incoherent (diffusive) channels. This model can reconcile the disagreement in the explanation of the primary process in rhodopsin between the two earlier works done by the two groups.[14,15] The shorter (<200 fs)[14] and longer (400 fs)[15] isomerization time correspond to isomerization in rhodopsin and thermalization in bathorhodopsin, respectively, as shown in Figure 11.

Acknowledgment. The authors express gratitude to Drs. M. Yoshizawa and K. Misawa for their helps in femtosecond experiments of rhodopsin and halorhodopsin, respectively. The authors also thank Drs. S. Hughes and B. Ullrich for careful reading of the manuscript.

References and Notes

(1) Yoshizawa, T.; Kito, Y. *Nature* **1958**, *182*, 1604.
(2) Yoshizawa, T.; Wald, G. *Nature* **1963**, *197*, 1279.
(3) Buchert, J.; Stefancic, V.; Doukas, A. G.; Alfano, R. R.; Callender, R. H.; Pande, J.; Akita, H.; Balogh-Nair, V.; Nakanishi, K. *Biophys. J.* **1983**, *43*, 279.
(4) Horiuchi, S.; Tokunaga, F.; Yoshizawa, T. *Biochim. Biophys. Acta.* **1980**, *591*, 445.
(5) Eyring, G.; Curry, B.; Mathies, R.; Fransen, R.; Palings, I.; Lugtenburg, J. *Biochemistry* **1980**, *19*, 2410.
(6) Shichida, Y.; Yoshizawa, T.; Kobayashi, T.; Ohtani, H.; Nagakura, S. *FEBS Lett.* **1977**, *80*, 214.
(7) Shichida, Y.; Kobayashi, T.; Ohtani, H.; Yoshizawa, T.; Nagakura, S. *Photochem. Photobiol.* **1978**, *27*, 335.
(8) Kobayashi, T. *FEBS Lett.* **1979**, *106*, 313.
(9) Kobayashi, T. *Photochem. Photobiol.* **1980**, *32*, 207.
(10) Matsuoka, S.; Shichida, Y.; Yoshizawa, T. *Biochem. Biophys.* **1984**, *765*, 38.

(11) Ohtani, H.; Kobayashi, T.; Tsuda, M.; Ebrey, T. G. *Biophys. J.* **1988**, *53*,17.
(12) Shichida, Y.; Matsuoka, S.; Yoshizawa, T. *Photobiochem. Photobiophys.* **1984**, *7*, 221.
(13) Taiji, M.; Bryl, K.; Nakagawa, M.; Tsuda, M.; Kobayashi, T. *Photochem. Photobiol.* **1992**, *56*, 1003.
(14) Schoenlein, R. W.; Peteanu, L. A.; Mathies, R. A.; Shank, C. V. *Science* **1991**, *254*, 412.
(15) Yan, M.; Manor, D.; Weng, G.; Chao, H.; Rothberg, L.; Jedju, T. M.; Alfano, R. R.; Callender, R. H. *Pros. Natl. Acad. Sci. U.S.A.* **1991**, *88*, 9809.
(16) Schoenlein, R. W.; Peteanu, Wang, Q. W.; S. J.; Mathies, R. A.; Shank, C. V. Proceedings Ultrafast Phenomena VIII. *Chem. Phys.* **1993**, *55*, 53.
(17) Oesterhelt, D.; Stoeckenius, W. *Proc. Natl. Acad. Sci. U.S.A.* **1973**, *70*, 2853.
(18) Schobert, B.; Lanyi, J. K. *J. Biol. Chem.* **1982**, *257*, 10306.
(19) Stoeckenius, W.; Lozier, R. H.; Bogomolni, R. A. *Biochim. Biophys. Acta.* **1979**, *505*, 215.
(20) Kandori, H.; Yoshihara, K.; Tomioka, H.; Sasabe, H. *J. Phys. Chem.* **1992**, *96*, 6066.
(21) Polland, H. J.; Franz, M. A.; Zinth, W.; Kaiser, W.; Hegemann, P.; Oesterhelt, D. *Biophys. J.* **1985**, *47*, 55.
(22) Kandori, H.; Yoshihara, K.; Tomioka, H.; Sasabe, H. *Chem. Phys. Lett.* **1991**, *187*, 579.
(23) Zimányi, L.; Keszthelyi, L.; Lanyi, J. K. *Biochemistry* **1989**, *28*, 5165.
(24) Fodor, S. P. A.; Bogomolni, R. A.; Mathies, R. A. *Biochemistry* **1987**, *26*, 6775.
(25) Zimányi, L.; Lanyi, J. K. *Biochemistry* **1989**, *28*, 1662.
(26) Lanyi, J. K.; Vodyanoy, V. *Biochemistry* **1986**, *25*, 1465.
(27) Oesterhelt, D.; Hegemann, P.; Tittor, J. *EMBO J.* **1985**, *4*, 2351.
(28) Duschl, A.; McCloskey, M. A.; Lanyi, J. K. *J. Biol. Chem.* **1988**, *263*, 17016.
(29) Tittor, J.; Oesterhelt, D.; Maurer, R.; Desel, H.; Uhl, R. *Biophys. J.* **1987**, *52*, 999.
(30) Rothschild, K. J.; Bousché, O.; Braiman, M. S.; Hasselbacher, C. A.; Spudich, J. L. *Biochemistry* **1988**, *27*, 2420.
(31) Lanyi, J. K.; *Physiol. Rev.* **1990**, *70*, 319.
(32) Mathies, R. A.; Brito Cruz, C. H.; Pollard, W. T.; Shank, C. V. *Science* **1988**, *240*, 777.
(33) Dobler, J.; Zinth, W.; Kaiser, W.; Oesterhelt, D. *Chem. Phys. Lett.* **1988**, *144*, 215.
(34) Kobayashi, T.; Terauchi, M.; Kouyama, T.; Yoshizawa, M.; Taiji, M. *Laser Applications in Life Sciences, Part two: Lasers in Biophysics and Biomedicine*; SPIE: Bellingham, WA, 1990; Vol. 1403, pp 407.
(35) Polland, H. J.; Franz, M. A.; Zinth, W.; Kaiser, W.; Kölling, E.; Oesterhelt, D. *Biophys.* J. **1986**, *49*, 651.
(36) Zimányi, L.; Ormos, P.; Lanyi, J. K. *Biochemistry* **1989**, *28*, 1656.
(37) Pollard, W. T.; Dexheimer, S. L.; Wang, Q.; Peteanu, L. A.; Shank, C. V.; Mathies, R. A. *J. Phys. Chem.* **1992**, *96*, 6147.
(38) Tallent, J. R.; Hyde, E. W.; Findsen, L. A.; Fox, G. C.; Birge, R. R. *J. Am. Chem. Soc.* **1992**, *114*, 1581.
(39) Doukas, A. G.; Junnarkar, M. R.; Alfano, R. R.; Callender, R. H.; Kakitani, T.; Honig, B. *Proc. Natl. Acad. Sci U.S.A.* **1984**, *81*, 4790.
(40) Yoshizawa, M.; Taiji, M.; Kobayashi, T. *IEEE J. Quantum Electron.* **1989**, *25*, 2532.
(41) Kobayashi, T.; Yoshizwa, M.; Stamm, U.; Taiji, M.; Hasegawa, M. *J. Opt. Soc. Am.* **1990**, *B7*, 1558.
(42) Sharkov, A. V.; Pakulev, A. V.; Chekalin, S. V.; Matveetz, Y. A. *Biochim. Biophys. Acta* **1985**, *808*, 94.
(43) Gai, F.; Hassan, K. C.; Anfinrud, P. A. Proceedings Ultrafast Phenomena, 1996. *Techn. Dig. Ser.* **1996**, *8*, 280.
(44) Peteanu, L. A.; Schoenlein, R. W.; Wang, Q.; Mathies, R. A.; Shank, C. V. *Proc. Natl. Acad. Sci. U.S.A.* **1993**, *90*, 11762.
(45) Landau, L. D. *Phys. Z. Sowjetunion* **1932**, *2*, 46.
(46) Zener, C. *Proc. R. Soc. London* **1932**, *A137*, 686.
(47) Kayanuma, Y. *J. Phys. Soc. Jpn.* **1984**, *53*, 108.